Transactions of the Royal Society of Edinburgh: Earth Sciences, **87**, 23–31, 1996

Dynamic model of dehydration melting motivated by a natural analogue: applications to the Ivrea–Verbano zone, northern Italy

Scott A. Barboza and George W. Bergantz

ABSTRACT: Dehydration melting of crustal rocks may commonly occur in response to the intrusion of mafic magma in the mid- or lower crust. However, the relative importance of melt buoyancy, shear or dyking in melt generation and extraction under geologically relevant conditions is not well understood. A numerical model of the partial melting of a metapelite is presented and the model results are compared with the Ivrea–Verbano Zone in northern Italy. The numerical model uses the mixture theory approach to modelling simultaneous convection and phase change and includes special ramping and switching functions to accommodate the rheology of crystal–melt mixtures in accordance with the results of deformation experiments. The model explicitly includes both porous media flow and thermally and compositionally driven bulk convection of a restite-charged melt mass. A range of melt viscosity and critical melt fraction models is considered. General agreement was found between predicted positions of isopleths and those from the Ivrea–Verbano Zone. Maximum melt velocities in the region of porous flow are found to be 1×10^{-7} and 1×10^{-1} m per year in the region of viscous flow. The results indicate that melt buoyancy alone may not be a sufficient agent for melt extraction and that extensive, vigorous convection of partially molten rocks above mafic bodies is unlikely, in accord with direct geological examples.

KEY WORDS: melt segregation, partial melting, convection, mixture theory, underplating, phase change, critical melt fraction, lower crust, Ivrea Zone.

Many continental granitoids contain at least some component of crustally derived material (Wyllie 1977; Pitcher 1993; Brown 1994; Harris *et al.* 1995). One mechanism for generating crustal melts is dehydration melting following the ponding of mantle-derived magma within or at the base of the crust (Huppert & Sparks 1988; Bergantz & Dawes 1994). Of particular interest is the melting of pelitic rocks, as there is ample field evidence for this process during contact metamorphism (Grant & Frost 1990; Harris *et al.* 1995; Symmes & Ferry 1995). However, little is known about the rates of melt generation and mechanisms of melt transport. Some studies have indicated that melt may be removed from the source region through an efficient mechanism. For example, in the Ballachulish aureole, granitic melt appears to have segregated into leucosomes in less than 5×10^4 years (Buntebarth 1991; Sawyer 1994). Sawyer (1991) proposed that tonalitic melt in the Grenville front probably separated from its source in less than 100 years.

Clemens and Mawer (1992) have argued that the mechanism for melt removal may be fracturing resulting from the positive ΔV of hydrate breakdown during dehydration melting, whereas other studies have emphasised the role of deformation and shear (Sawyer 1994; Brown *et al.* 1995; Davison *et al.* 1995; Rushmer 1995). Melt segregation in the mantle, on the other hand, is thought to result primarily from buoyancy forces which initiate the porous flow of melt (Nicolas 1989). It is likely that each of these mechanisms (fracturing, shear and buoyancy), to some extent, contributes to the extraction of crustal melts from their source. However, the relative importance of buoyancy or shear in the melt transport process is poorly understood.

The thermal evolution of underplating regions has also been a subject of much debate. Analogue experiments and mathematical models have led to the proposal that underplating of basaltic magmas will lead to bulk melting of the country rock and the thermal evolution of underplating regions will be dominated by convective processes (Huppert & Sparks 1988). However, there is little direct geological or geochemical evidence to support this view. As a result, the style and vigour of convection in both the basaltic sill and the overlying country rock have been subject to much debate (Huppert & Sparks 1991; Marsh 1991) and numerous alternative models have been advanced (Bergantz & Dawes 1994).

One of the central themes of this study is that rheological variations associated with the increase in melt fraction during melting provides the dominant control on the dynamics of the growing region of partial melt. The notion of a distinct critical melt fraction (CMF), at which the skeleton of restitic crystals breaks down and stresses are supported by the fluid phase, requires substantial revision for geological systems undergoing partial melting. The rheological transitions in partially molten rocks can be complex and difficult to generalise (Rushmer 1995; Rutter & Neumann 1995). The rheological model invoked in this study is an extension of mixture theory for two-phase systems (Agarwal & O'Neill 1988; Ni & Beckermann 1991; Oldenburg & Spera 1992). The CMF can still play a part in the rheological characterisation of partially molten material, but it does not represent an abrupt transition from a rigid skeleton to a crystal-laden fluid, but rather a gradual transition between the two.

The intent of this study is to explore the relationship between melt generation, the dynamics of melt movement and the thermal evolution of an underplated region adhering to documented geological conditions. To this end a thermo-

mechanical model has been developed: (1) to explore the time and length scales of dehydration melting and the dynamics of melt movement following underplating; and (2) to evaluate the influence of thermally and compositionally induced buoyancy as a mechanism for the extraction of felsic melt. A numerical study is particularly well suited to address such questions as experiments carried out with laboratory analogues cannot be used to assess the relative importance of such processes in a physically realistic manner (Bergantz & Dawes 1994; Bergantz 1995; Jaupart & Tait 1995). A similar modelling approach has been used by Irvine (1970), Bergantz (1989) and Bowers *et al.* (1990) for evaluating partial melting during contact metamorphism. However, these studies allowed no convection in the region of partial melting and cannot resolve issues related to the dynamics of melt movement.

The geometrical and thermal relationships used in this study are based on current models for the emplacement dynamics of the underplated igneous complex at the Ivrea–Verbano Zone (IVZ) (Quick *et al.* 1994). A simplified version of this process is summarised in Figure 1. Mantle-derived magma near its liquidus temperature (1200°C) is emplaced in a small, spatially stable sill at the base of an initially unmelted sequence of pelitic rocks in the lower crust. The growth of a solid, conductive quenched margin causes the contact to stabilise at a temperature intermediate between that of the country rock and the initial temperature of the intruding basalt. Melting in the country rock proceeds as the intrusion cools and buoyant instabilities develop in the growing lens of felsic melt. The movement of melt that results from these instabilities advects heat away from the contact with the intrusion and yields a region of partial melting whose geometry and rate of growth differs significantly from both conductive models and those that assume convection is turbulent.

1. The Ivrea–Verbano Zone: a field example

The results of this study will be compared with the IVZ in northern Italy, arguably the premier locality for the study of dehydration melting subsequent to underplating. The IVZ (Fig. 2) is a lower crustal section consisting of a 140 km long sequence of steeply dipping pelitic and mafic rocks metamorphosed under amphibolite to granulite facies conditions (Zingg 1980). To the NW, the IVZ is separated from rocks of the

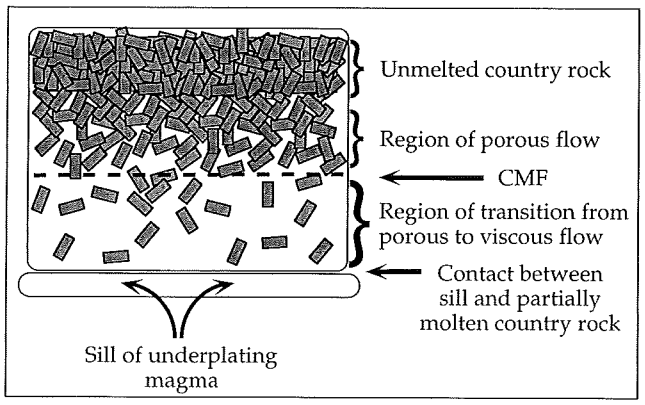

Figure 1 Schematic diagram for melting model. A sill of mantle-derived magma is intruded at the base of a sequence of pelitic rocks. Heat transfer to the sequence causes partial melting of the pelitic rocks and results in buoyant instabilities in the pelite–melt mixture. These instabilities cause the upwards flow of material from the region near the contact with the sill, further enhancing the heating and melting of the pelitic sequence above. When the local volume fraction of melt exceeds the critical melt fraction (CMF), the rheological transition between the porous and viscous flow end-member rheological regimes is initiated.

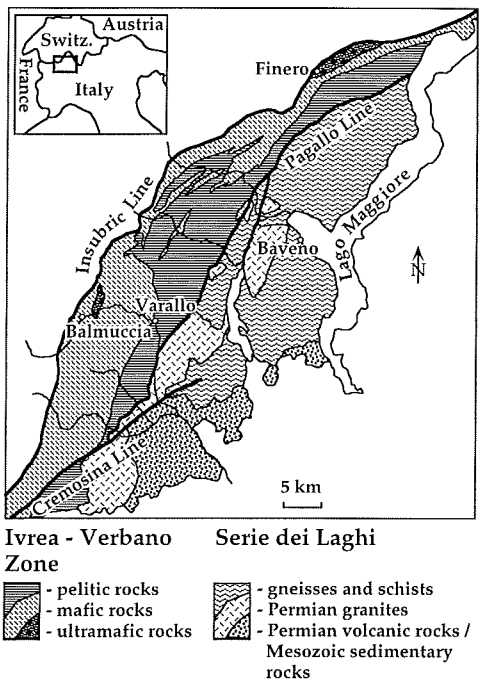

Figure 2 Geological sketch map of the southern Alps west of the Lago Maggiore (modified from Zingg 1980). Inset shows location of area in northern Italy.

Austroalpine Domain by the Insubric Line—a major shear zone that marks the southern extent of Alpine deformation (Schmid *et al.* 1987). To the SE, the IVZ is separated from rocks of intermediate crustal depth within the Serie dei Laghi unit by the Cremosina and Pogallo Lines (Boriani *et al.* 1977, 1988; Zingg 1983).

The IVZ is composed of two major lithologic divisions—the Kinzigite Formation and the Mafic Complex. The Mafic Complex is primarily composed of rocks of gabbroic composition, but also includes large peridotite bodies near the Insubric Line and dioritic rocks near the contact with the Kinzigite Formation (Rivalenti *et al.* 1975, 1980; Sinigoi *et al.* 1994). The Kinzigite Formation is composed predominantly of sillimanite-bearing paragneisses termed 'kinzigites' and 'stronalites' in the amphibolite and granulite grade, respectively (Zingg *et al.* 1980). The rocks of the Kinzigite Formation were exposed to increasingly higher degrees of metamorphism towards the contact with the Mafic Complex and, importantly, are increasingly depleted in the granitophile elements with increasing degree of metamorphism (Schmid & Wood 1976; Schmid 1978/79). Together, the IVZ and the Serie dei Laghi are thought to represent an uplifted cross-section through the continental crust (Mehnert 1975; Fountain 1976).

2. Dehydration melting

The melting relationships used in this model are that of the fluid-absent (dehydration) melting of metapelitic rock. Dehydration melting is defined as the melt reaction that occurs when all of the water in the system is initially contained within the hydrous mineral assemblage and is transferred directly to the melt during the melting reaction without ever appearing as a product or reactant (Rushmer 1991). There are numerous studies which emphasise the importance of this process for crustal growth and evolution (Brown & Fyfe 1970; Thompson 1982; Yardley 1986; Whitney 1988; Beard & Lofgren 1989). We choose to focus on dehydration melting in this study because it has been suggested as: (1) a major source of contamination in intruding mafic magmas (e.g. Sinigoi *et al.*

1994); (2) a source of migmatites and other water-undersaturated granitic melts (Rushmer 1991); (3) a cause of some granulite formations (Mehnert 1968; Fyfe 1973; Wickham 1987); and (4) a source of melts of tonalitic to trondhjemitic composition (Rushmer 1991).

3. Methodology

3.1. General nature of melt movement

A region undergoing melting is essentially a solid–liquid mixture with multiple phase changes. Unlike a pure substance, there is no distinct crystallisation front; rather the solid melts over a temperature range (Fig. 1). Mixture theory provides an approach for the development of the equations describing the transport of energy, mass, momentum and chemical species. A comprehensive discussion of the theory and derivation of the full set of continuum governing equations is discussed in detail elsewhere and will not be revisited here (Bennon & Incropera 1987; Prakash & Voller 1989; Oldenburg & Spera 1991). A detailed discussion with regards to the derivation and specific application is given in Barboza (1995). The key feature of the mixture theory approach is that it explicitly allows for the full range of dynamic conditions, from porous media flow at low melt fraction to fully liquid behaviour at high melt fraction.

The melt fraction at which the solid skeleton breaks down and the flow regime changes from one of porous flow to that of viscous flow with suspended solids is the CMF. The fraction of melt is less than the CMF in the region of porous flow where the solid skeleton is considered to be fixed relative to the percolating interstitial melt. A wide range of estimates for the CMF of a number of compositions are available. Experimental deformation of partially molten granite yields estimates of CMF$\approx$25–30% (Arzi 1978; van der Molen & Paterson 1979). Estimates based on the distribution of the phenocryst content of erupted lava and theoretical arguments based on contiguity limits yield more conservative estimates of CMF$\approx$50% (Marsh 1981; Miller *et al.* 1988). However, the experiments of Rutter and Neumann (1995) produced no sharp discontinuity in strength with increasing melt fraction. In light of this result, we have used a ramping, switching function to model the transition in drag from Darcy-dominated drag to suspension-dominated drag (Figure 3). Hence the transition from Darcy-dominated porous to suspension-dominated viscous flow did not occur at a distinct value of the CMF. References to the CMF in this study should be understood to be a reference melt fraction at which the transition to suspension-dominated flow is initiated, not as indicating an abrupt transition in rheology. Other rheological models could have been chosen; our choice reflects a best estimate taken from current experimental results. The permeability in the region of porous flow was calculated using the Blake–Carmen–Kozeny relation.

Melt movement in both the porous flow and viscous flow regime was initiated by buoyant instabilities that arise from variations in the density of the melting pelite. These density changes are strongly dependent on the distribution of suspended solids, the melt composition and the temperature. The magnitude of the buoyancy force resulting from these density changes is incorporated in the thermal and solutal expansion coefficients in the buoyancy source term for the momentum equation. The expansion coefficients were derived from the experimental data with calculations using the MELTS algorithm (Ghiorso & Sack 1995).

The melt viscosity was calculated from the experimental data by the Shaw model (Shaw 1972) and the Krieger and Dougherty relation was used to account for the influence of

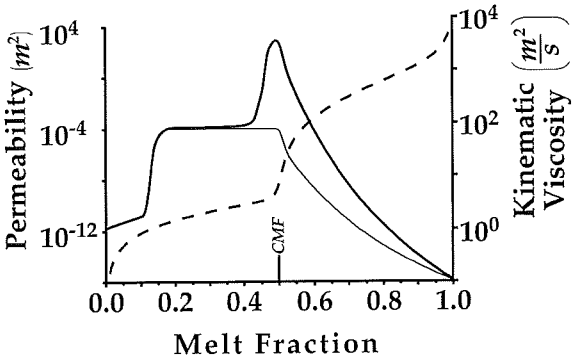

Figure 3 Plot of the kinematic viscosity (solid lines) and permeability (broken line) as a function of the melt fraction. The thin solid line gives the variation of the viscosity of the melt only and the thick solid line is the model mixture viscosity, which includes the influence of suspended solids. The low viscosity at low melt fractions arises because of the high water content of the experimental melts (Vielzeuf & Holloway 1988). The critical melt fraction (CMF) is the melt fraction at which the transition from porous to viscous flow is initiated. The CMF, in this instance, is 0·5. Simulations using different values for CMF had qualitatively similar relationships.

suspended solids (Wildemuth & Williams 1984; Oldenburg & Spera 1992; Bergantz & Dawes 1994). As with permeability, a switching function has been incorporated in the viscosity relation to ensure that the influence of suspensions does not affect the effective viscosity in the region of porous flow (Oldenburg & Spera 1992). Figure 3 depicts the kinematic viscosity as a function of melt fraction for the melt and for the magma (melt+solid suspensions). The temperature and composition dependence of the viscosity of the melt was calculated from the experimental melt compositions and temperatures as a function of the observed melt fractions and, therefore, assumes equilibrium melting (Vielzeuf & Holloway 1988). The melt viscosity is constant between melt fractions of 0·15 and 0·5 because the melt generated within this range takes place at the biotite dehydration invariant point, so temperature and composition do not change. The large increase in effective viscosity just above the CMF approximates the influence of suspended solids on the viscosity of the magma during viscous flow. Although the Krieger and Dougherty relation yields excellent agreement with experimental data (Wildemuth & Williams 1984), some work has demonstrated that, under certain conditions, the Shaw model may overestimate the viscosity of a silicate melt by up to two orders of magnitude (Schulze *et al.* 1994). Thus the model simulations were conducted using the entire range of proposed felsic melt viscosities.

3.2. Thermodynamic model

The modelling strategy adopted in this study is that of mixture theory where the multi-phase governing equations are averaged, yielding a single set of governing equations for the melt–restite mixture. Closure of these governing equations for the solid–liquid mixture requires that additional thermodynamic functions be developed to link the enthalpy and composition to the melt fraction. By assuming local equilibrium, the phase diagram provides the necessary relationships.

The dehydration melting of both muscovite and biotite (neglecting the influence of biotite solid solution) takes place at invariant points. The composition of the melt produced at these invariant points will remain constant as long as the restitic phases are in equilibrium with the invariant point melt composition. In addition, excess alumina and mafic oxides have very low solubilities in melts dominated by the orthoclase and H_2O components. The particular mica composition

undergoing melting will therefore influence the composition of the restitic phases, but have only a limited influence on the composition of the melt (Patiño Douce & Johnston 1990). As the composition of the melt produced during the dehydration melting of either mica is approximately the same, the melt generated at either invariant point and the suite of resulting restite compositions define a line within the compositional volume. Removal of this melt will cause the composition of the remaining unmelted restite to evolve linearly (Patiño Douce, pers. comm.) and a simple pseudo-binary phase diagram may capture much of the melting systematics of some pelitic rocks. Errors in melt fraction estimates resulting from this approximation will be minimal at the relatively low temperatures of interest where the refractory phases are not involved in the melting reaction. In addition, smaller errors are expected for pelite compositions in which melting occurs dominantly at one or the other of the invariant points.

The pelite composition used in the experiments of Vielzeuf and Holloway (1988), in which melting takes place predominately by biotite dehydration melting, was selected as our model composition. Three benefits are obtained by choosing this particular pelite. Firstly, as discussed earlier, errors in the predicted melt composition will be minimised when most of the melting occurs at an invariant point. Secondly, this composition is optimum for melt production. By 'optimum', we mean that this composition produces more melt at lower temperatures than most naturally occurring crustal rocks (Bergantz & Dawes 1994). This composition provides a useful end-member for evaluating the general dynamics of melt production and extraction in the lower crust. Finally, the composition corresponds reasonably well to the average metagreywacke composition found in the Kinzigite Formation of the IVZ (Schnetger 1994). The major difference in mineralogy is that the Kinzigite Formation metagreywacke contains 6% K-feldspar and 3% muscovite, whereas the experimental pelite composition contains 0 and 9%, respectively, of these minerals.

3.2.1. Building the binary. The first step in the thermodynamic parameterisation is to build a pseudo-binary from which to generate liquid fraction and composition data. The 10 kbar NKM (Na_2O·Al_2O_3–K_2O·Al_2O_3–MgO + FeO)-, silica-, alumina-, titania-saturated pseudo-ternary (Fig. 4) was chosen on which to plot the experimental melt compositions. The phase relations, invariant points and cotectics were derived by Patiño Douce and Johnston (1990) using their own data with those of Vielzeuf and Holloway (1988) and Le Breton and Thompson (1988). We observe that the suite of melt compositions along with the invariant points form an approximately linear array across this pseudo-ternary. Our methodology was to extend a binary from the M apex of the pseudo-ternary through the array of compositions and invariant points to the intersection with the N–K join (M′). The experimental melt compositions and derived invariant points were then projected onto the binary join and composition was parameterised as a fractional distance along the pseudo-binary. The liquidus line was constrained by the projected experimental melt compositions and the temperatures at which they were generated. The solidus line was derived using the lever rule by fitting the variation of liquid fraction with temperature observed in the experiments and calculated from mass balance with that predicted by the model (Fig. 5).

3.3. Model description

We consider melting of a sequence of pelitic rocks in the two-dimensional, 5 km × 5 km computational domain overlying the contact with a sill of basaltic magma in the lower crust. The geometry of the sill underlying the computational domain

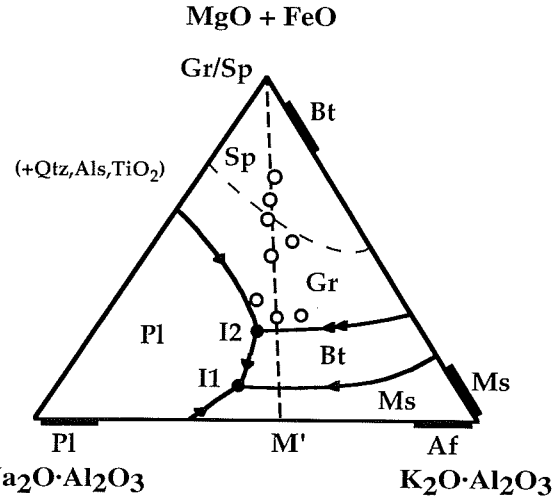

Figure 4 10 kbar NKM-, silica-, alumina- and titania-saturated pseudo-ternary liquidus phase relations projected from the KNMH volume (Patiño Douce & Johnston 1990). Closed circles are the biotite dehydration invariant point (I2) and the muscovite dehydration invariant point (I1). Open circles are the projections of the Vielzeuf and Holloway (1988) experimental liquid compositions. Thick broken line between the MgO + FeO apex and M′ is the pseudo-binary used in the model. Mineral abbreviations: Sp = spinel; Gr = garnet; Pl = plagioclase feldspar; Af = alkali feldspar; Ms = muscovite; Qtz = quartz; Als = aluminosilicate; Bt = biotite.

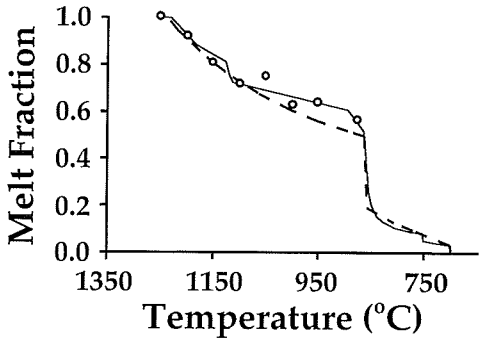

Figure 5 Predicted variation of melt fraction as a function of temperature using a lever rule formulation and the phase relationships depicted in Figure 4. Broken line is the model melt fraction curve; the solid line is that calculated by Vielzeuf and Holloway (1988) using inferred melting relationships. The open circles are the melt fractions observed in the melting experiments (Vielzeuf & Holloway 1988).

was based on current estimates of the sill width during emplacement of the Mafic Complex at the IVZ (Quick *et al.* 1994). The sill was stipulated to be 2 km in width and long enough that the important features of the convection could be captured in two dimensions (Fig. 1). No assumption was made about the sill thickness except that it contained enough basaltic magma to maintain the contact temperature throughout the duration of the simulations. This will be addressed in more detail in the following.

The computational domain was oriented such that the right wall was parallel to the vertical plane of symmetry of the sill (Fig. 1). The results thus depict melting in a semi-infinite half-space over one limb of the intruding sill. A 65 × 65 variable spaced grid was used and the domain was separated into regions for the purposes of grid point distribution. The highest density of nodes was placed in a 2 km × 2 km region surrounding the simulated contact with the sill. All simulations were halted before the melting front left the region of higher resolution grid spacing. A grid refinement study was also undertaken to ensure that the solutions were independent of spatial and temporal grid spacing.

At time $t=0$, the temperature along the base of the computational domain up to 1 km from the right-hand wall was elevated to a value of $T_{contact}$, simulating the intrusion of a 2 km wide sill of underplating mafic magma. The contact temperature was maintained through the duration of the simulations. The other walls of the domain were insulated, but all simulations were halted before an appreciable increase in temperature (1–5°C) was observed at the roof or left wall. This ensured that the thermal boundary conditions did not significantly influence the solution. No-slip boundary conditions were used on the left wall, roof and floor. Free-slip conditions were allowed on the right wall as it was the axis of symmetry of melt movement.

The material in the domain was initially the unmelted fertile pelite composition of Vielzeuf and Holloway (1988). The initial pressure and temperature in the domain were 10 kbar and 600°C—about 150°C below the solidus of the model composition pelite and corresponding to the approximate depth at which the Mafic Complex was probably intruded (Zingg 1983). These conditions correspond to a relatively high continental geotherm (17°C/km), but are similar to predicted geotherms for modern underplating regions such as in NE Japan and the Rio Grande Rift (Kay & Kay 1980; Hyndman 1981). Two sets of simulations (case 1 and case 2) were performed using different contact temperatures ($T_{contact}$) over the range of estimates for these rheological parameters. A summary of the different combinations of $T_{contact}$ and rheological parameters used in the simulations is given in Table 1, along with the other model thermo-physical properties.

Table 1 Data for the model.

Property (units)	Numerical value
Property data	
Specific heat (J/kg K)	$1{\cdot}04\times10^{3}$
Thermal conductivity (W/m K)	1·9
Density (kg/m^3)	$2{\cdot}507\times10^{3}$
Kinematic viscosity (m^2/s)	See text
Schmidt number (μ^l/D)	$1{\cdot}0\times10^{6}$
Latent heat (J/kg)	$1{\cdot}0\times10^{5}$
Permeability coefficient (m^2)	$5{\cdot}56\times10^{-10}$
Thermal expansion coefficient (K^{-1})	$1{\cdot}05\times10^{-4}$
Solutal expansion coefficient (C^{-1})	$1{\cdot}55\times10^{-1}$
Initial conditions	
Pelite starting composition	0·325
Initial temperature (°C)	600·0
Contact temperatures and rheological parameters used in simulations	
Contact temperature (°C)	Case 1 = 1000·0
	Case 2 = 900·0
Range of CMF	0·35, 0·4, 0·45, 0·5, 0·55
Range of μ^l/μ^l_{Shaw}*	1·0, 0·5, 0·1, 0·01

* μ^l/μ^l_{Shaw} is the ratio of the melt viscosity used in the simulations to that predicted by the Shaw model using MELTS.

4. Results and discussion

4.1. Thermal evolution and the distribution of melt above the underplating sill

The vigour of convection and the amount of melt produced in the pelite was found to be strongly dependent on $T_{contact}$ and the combinations of values for the rheological parameters of the system (CMF and μ^l/μ^l_{Shaw}). Note that μ^l/μ^l_{Shaw} is the viscosity of the melt used by a particular simulation divided by the viscosity predicted by the Shaw model. A simple way of evaluating the convective vigour is by monitoring the evolution of the melt distribution in the partially molten pelite above the sill and by comparing the melt distribution for simulations with different values of $T_{contact}$ and the rheological parameters. We use profiles of the melt distribution rather than the total mass of melt to emphasise the field comparison because the model pelite composition exhibits large jumps in melt fraction which correspond with the disappearance of easily recognisable minerals from the assemblage. The profiles are monitored along the right wall of the computational domain and three cases are presented for comparison (Fig. 6). Plot A is a case 1 ($T_{contact}=1000$°C) simulation in which the convection was observed to be vigorous relative to the other simulations. Plot B (case 1) and plot C (case 2) are both simulations in which convection was suppressed. The sharp increase in melt fraction furthest from the contact with the sill is caused by muscovite dehydration melting. The second large increase in melt fraction closer to the contact is biotite dehydration. The spatial position of the muscovite-out (I1) and biotite-out (I2) transitions are labelled on plot B.

Note that in the case 1 simulations the distance the biotite-out transition had propagated from the contact was strongly dependent on the presence of convection. The distance the muscovite-out transition had propagated, on the other hand,

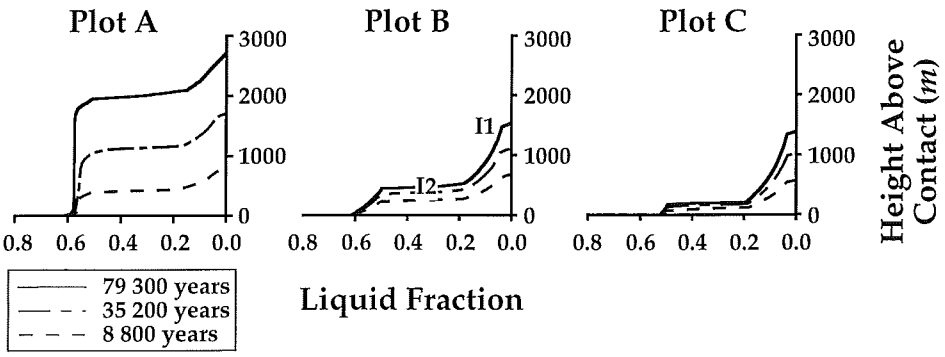

Figure 6 Evolution of melt distribution. Plot A is a plot of the distribution of melt within the pelite–melt mixture with height above the apex of the underplating sill during a convection-dominated simulation. Plot A is a case 1 simulation (see text) in which $\mu^l/\mu^l_{shaw}=0{\cdot}1$ and CMF = 0·45. Three curves are shown in plot A depicting the melt fraction at different times during the simulation. Plots B and C are conduction-dominated simulations from cases 1 and 2, respectively. The sharp increase in melt fraction furthest from the contact is the location of the muscovite melting reaction (11). The second large increase in liquid fraction closer to the contact is that of the biotite melting reaction (12). The position of the invariant points is labelled on one curve in plot B or reference. CMF = critical melt fraction; μ^l/μ^l_{shaw} is the viscosity used in a particular simulation divided by the calculated viscosity using the Shaw model.

was relatively unaffected by advective transport of heat through most the duration of the simulations. For instance, in the presence of convection after $3{\cdot}5 \times 10^4$ years (plot A in Fig. 6), muscovite was no longer stable in the assemblage at a height of about 1·6 km above the contact with the sill. The position of the muscovite-out isograd is about 1·1 km in the conduction case—only 0·5 km closer to the contact. The biotite-out transition, on the other hand, had propagated 1·2 km from the contact with the intrusion in the convective case (plot A), but only 0·4 km in the conduction case (plot B). We conclude that, in the field, the muscovite-out transition will probably lie relatively close to a conductive isotherm whether or not buoyancy-driven melt movement was an important component of the thermal evolution of the region.

In the IVZ, the muscovite-out isograd lies approximately 1 km stratigraphically above the contact with the Mafic Complex (Zingg 1980) in the vicinity of what is believed to be the locus of the intrusion (Quick *et al.* 1994). The simulations demonstrate that, even with the lowest rates of heat flux to the country rock overlying the sill (plot C), the muscovite-out transition will propogate 1 km after only $3{\cdot}5 \times 10^4$ years. The exposed portion of the Mafic Complex south of Val Strona di Omegna covers an area of over 350 km^2 (Fig. 2) and geophysical studies indicate that the complex may project many tens of kilometres into the crust (Giese 1968; Kissling 1980; Zingg 1983). These observations appear to require the unlikely combination of extremely high magma supply rates to the mafic complex (higher than 0·4 km^3 per year), coupled with limited heating of the overlying country rock, as indicated by the relatively short distance the muscovite-out transition propagated from the contact. For comparison, estimates of the average effusion rates for Hawaii and the Columbia River Basalt Group are of the order of 0·1 km^3 per year (Swanson *et al.* 1989). We believe that it is more likely that the temperature of the overlying country rock reached a steady-state temperature lower than might be expected given the volume of magma that made up the Mafic Complex. This indicates that magmatism during the emplacement of the Mafic Complex was probably episodic, punctuated by long periods of stagnation.

4.2. Convective velocities and the rheological and thermal envelope of convection

A more rigorous evaluation of convective vigour was undertaken by monitoring the time evolution of the heat absorption ratio (H_{abs}). H_{abs} is defined as the total amount of latent and sensible heat absorbed by the system (H_{conv}) in the presence of convection relative to that calculated by a simulation performed under the same conditions in which the heat transfer was forced to occur by conduction only (H_{cond}).

$$H_{abs} = \frac{H_{conv}}{H_{cond}}$$

For the purposes of discussion, simulations in which $H_{abs} = 1$ were termed 'conduction-dominated' as conduction was the dominant mode of heat transfer in the system. Simulations in which $1 < H_{abs} < 2$ were termed 'convection-influenced' and those in which $H_{abs} \geq 2$ were termed 'convection-dominated' as the heat transfer in the presence of convection was at least twice that of conduction alone.

Convective velocities in all simulations in cases 1 and 2 were variable, but generally small. Maximum convective velocities in the region of porous flow were of the order of 1×10^{-7} m per year and porous flow transported an insignificant amount of heat. Maximum convective velocities in the region of viscous flow, on the other hand, were of the order of 1×10^{-1} m per year. Viscous flow was thus sufficient, in some simulations, to influence the thermal evolution. H_{abs} values larger than 5 were observed for simulations in which the rheological parameters were optimum for convection ($\mu^l/\mu^l_{shaw} = 0{\cdot}01$, CMF = 0·35) in case 1. Convective vigour, however, was dramatically less in case 2 simulations where the contact temperature was lower (900°C). In addition to the contact temperature, the influence of convection was observed to be a strong function of time, the CMF and the viscosity.

4.2.1. Influence of the rheological parameters on convective vigour. The influence of the contact temperature and rheological parameters on convective vigour can be illustrated by plotting H_{abs} over the range of estimates of the viscosity and the CMF 1×10^4 a after the initiation of the simulations (Fig. 7A).

Convective velocities high enough for the contact metamorphism to be convection-influenced are restricted to a limited range of estimates of the melt viscosity and CMF. More conservative estimates of these parameters tended to yield conduction-dominated solutions for all simulations in either case. Maximum magnitudes of convective velocities observed were approximately 1×10^{-1} m per year, but, more commonly, maximum magnitudes were between 1×10^{-5} and 1×10^{-3} m per year. Note, in particular, the dramatic decrease in convective vigour when the contact temperature was 900°C. Convection influenced the thermal evolution of only those case 2 simulations with the most optimum estimates of the rheological parameters ($\mu^l/\mu^l_{shaw} = 0{\cdot}01$ and CMF = 0·35). The contact temperatures used in the simulations (1000 and 900°C) are probably higher than in natural systems, so the weak convection observed in these simulations is probably more vigorous than to be expected in natural underplating regions. In general, buoyancy-driven convective stirring of a restite-charged, partially molten pelitic sequence is unlikely to occur. Such convection appears to require both extreme conditions of sustained, high-temperature magmatism and more optimum estimates of the rheological parameters.

4.2.2. Evolution of convective vigour with time. It is also informative to measure the time that elapsed before H_{abs} exceeded 1·0. We termed that period the 'convective rise time' and it was found to be strongly dependent on both the rheological parameters (viscosity and CMF) and the contact temperature ($T_{contact}$). Convective rise times were typically on the order of 1×10^3 a for case 1 and substantially longer (2–6×10^4 a) for case 2 (Fig. 7B).

These estimates should be taken as the minimum amount of time the contact temperature must be maintained to establish convection with sufficient vigour to influence the regional thermal evolution. Thus not only does vigorous convective stirring of the partially molten pelite require high contact temperatures and optimum estimates of the rheology, but it also requires a contact metamorphic event of significant duration. Buoyancy-driven viscous flow of partially molten country rock is likely to be isolated to regions experiencing long periods of sustained magmatism.

The minimum mass of basalt required to maintain the contact temperature through the duration of the convective rise time may be estimated by assuming that the composition of the basalt was that of a typical MORB and was intruded at a temperature of 1200°C and cooled to the contact temperature (1000 or 900°C). Latent heat released during crystallisation through this temperature range was accounted for by estimating the percentage crystallisation of the basalt with the MELTS algorithm (Ghiorso & Sack 1995). The mass of basalt was calculated by equating the amount of heat absorbed by the country rock with that released by the simulated intrusion (Fig. 7C). These values should be regarded as minimum estimates of the mass of basalt. In evaluating Fig. 7C, we might consider a sill about the dimensions of estimates of the size of mid-ocean ridge magma chambers

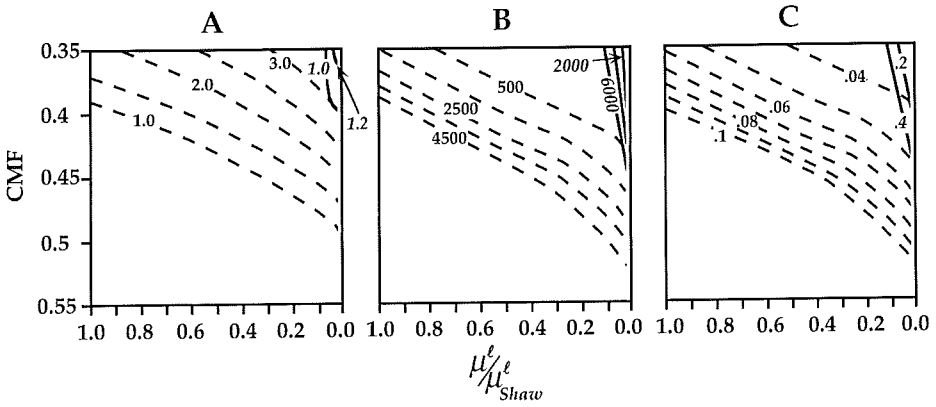

Figure 7 Contours of three parameters for case 1 ($T_{contact}=1000°C$) and case 2 ($T_{contact}=900°C$) simulations through the range of rheological parameters. Case 1 values are contoured by broken lines and case 2 values are plotted with solid lines with italicised contour labels. (A) Contours of the range of heat absorption ratios (H_{abs}) after $1{\cdot}0\times10^4$ years. Simulations in which $H_{abs}=1{\cdot}0$ were termed 'conduction-dominated', those with $1{\cdot}0<H_{abs}\{2{\cdot}0$ were termed 'convection-influenced', and those with $2{\cdot}0<H_{abs}$ were termed 'convection-dominated'. (B) Contours of the time (years) the contact temperature must be maintained for convection to become sufficiently vigorous to influence the regional thermal evolution. Weak convection was present, but was insufficiently vigorous to increase the amount of heat transferred to the unmelted pelite in conduction dominated simulations. (C) Contours of the minimum mass (in $kg/10^{10}$) of basalt per unit length of sill required to be intruded for convection in the pelite–melt mixture to become sufficiently vigorous to influence the thermal evolution of the domain. We assume the underplating cooled from the initial temperature of the intrusion (1200°C) to $T_{contact}$. Abbreviations as in Figure 6.

(Sinton & Detrick 1992). If we assume a sill 2 km in width and with a thickness of 100 m, it contains approximately 3×10^8 kg of basalt per metre of sill width in each limb. Cooling this amount of basalt would not yield the minimum amount of energy required to initiate the viscous flow of the partially molten sequence of pelitic rocks during the course of any simulation.

4.2.3. Application to the Ivrea-Verbano Zone. Temperatures of between 750 and 800°C have been estimated for the kinzigites and stronalites in the IVZ (Zingg 1983; Sills & Tarney 1984). It should be noted that these estimates place the temperature of the kinzigites close to that of the biotite dehydration reaction (12). Although the kinzigites near the contact with the Mafic Complex in Val Sesia have probably undergone a large degree of partial melting (Zingg 1980), they commonly retain a significant amount of biotite. It is thus unlikely that contact temperatures between the Kinzigite Formation and the underlying Mafic Complex were as high as 1000 or 900°C for significant periods of time. If the melting systematics of the model pelite are representative of the melting of a typical IVZ metagreywacke, the simulations indicate that it is likely that heat transport in both the kinzigites and stronalites was dominated by conduction and convection played a limited part in the transport of heat. In addition, given the relatively low temperatures indicated by the thermometry and the extremely limited convection observed in case 2 ($T_{contact}=900°C$) simulations, conduction is probable whether or not enough melt was produced to exceed the CMF.

4.3. Melt extraction

Convective velocities in the region of porous flow were insufficient to drive significant melt extraction during the course of any simulation. Maximum convective velocities observed in the region of viscous flow were about 1×10^{-7} m per year. The simulations were conducted over a period of 10^5 years so the maximum distance melt migrated from the source during the course of the simulations was of the order of centimetres. Given that the duration of a typical crustal melting event is of the order of 10^5–10^7 years (Sawyer 1994), the *maximum* distance that melt could be expected move within a partially molten pelite overlying a sill is probably less than a metre. These velocities are a maximum estimate because the contact temperature was held constant throughout the simulations. This cannot be the case in a natural underplating sill because, among other reasons, basalt would be nearly solidified and cooling conductively at 900°C and 10 kbar. The observed convective velocities are thus an end-member estimate of the natural system. In conclusion, the simulations indicate that the buoyancy of the melt alone is not sufficient to drive a significant extraction of melt from the porous skeleton. Deformation, fracturing or both may be the dominate mechanism for melt extraction in the continental crust and buoyancy-driven porous flow is, at best, a second-order process.

4.3.1. Existence of a low melt fraction window of extractable melt. In cases where melt extraction at low melt fraction (e.g. Sawyer 1994) is determined to be significant, it is possible to estimate from which region melt is most likely to be extracted. Given the non-linear variations in the viscosity (Fig. 3) of the melt residing within the porous skeleton, however, the propensity for melt extraction is unclear. Darcy's law implies that the propensity for melt extraction under a given pressure gradient can be estimated from the ratio of the permeability of the porous medium to the viscosity of the melt (K/μ^l) if melt movement is pervasive. Higher values of K/μ^l would indicate a higher propensity for melt extraction and K/μ^l should be directly proportional to the differential velocity between the melt and porous skeleton. A two order of magnitude increase in K/μ^l thus indicates a two order of magnitude increase in average differential velocities. A plot of K/μ^l with liquid fraction using the model permeability and viscosity relationships is shown in Fig. 8.

Melt existing in regions of a partially molten pelite that possess a melt fraction between 0·05 and 0·15 appears to have a relatively high propensity to undergo melt movement. In fact, the K/μ^l value predicted to exist within this melt fraction range is not exceeded until the system reaches a melt fraction of nearly 0·35. This melt fraction range was also correlated with a peak in the magnitudes of convective velocities in all simulations. Although the observed velocities were extremely small (1×10^{-7} m per year), the pressure gradient that

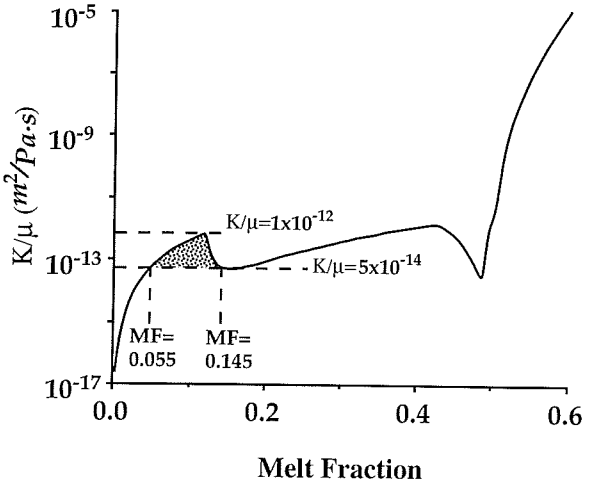

Figure 8 Plot depicting the relative propensity for melt movement within the porous skeleton as a function of the melt fraction. Higher values indicate a higher propensity for melt movement. Note that the values reached between melt fractions of 0·05 and 0·15 are not exceeded until after nearly 40% of the pelites has been melted. Stippled region is the 'low melt fraction window of extractable melt' discussed in the text. Broken lines are reference values.

generated the melt movement was due solely to the buoyancy of the melt and neglected other possible modes of transport. If, for example, dyking were to occur in the region, the velocity of the melt in the porous skeleton might be much higher. In such a circumstance we postulate that the melt existing in the range of melt fraction between 0·05 and 0·15 is the most likely to be extracted, barring the accumulation of a substantial percentage of melt (>40%) in the region.

5. Conclusions and summary

Phase relations for the dehydration melting of pelitic rocks have been parameterised for use in a thermo-mechanical model. Numerical simulations of the dehydration melting and subsequent buoyant melt migration of a sequence of pelitic rocks following the underplating of mafic magma in the lower crust have been performed. The total amount of melt produced is critically dependent on the dynamics of melt movement in the pelite–melt mixture.

Important factors influencing the vigour of melt and melt plus restite movement are the value of the CMF, viscosity and the temperature of the igneous contact. Recall that the CMF, as used in this study, does not provide an abrupt transition from porous-dominated to suspension-dominated drag. Instead, the CMF is a reference value for the initiation of this transition. Simulations in which conservative estimates of the CMF$\approx$0·5 and the melt viscosity calculated by the Shaw model were used tended to yield conduction-dominated solutions. Other estimates of the melt viscosity yielded weak convection that influenced the thermal evolution of crustal rocks to a varying degree.

The simulations demonstrate that vigorous convective stirring in the region of viscous flow and a significant amount of melt extraction within the porous skeleton will probably not occur except under extreme conditions (i.e. long, sustained periods of magmatism; large amounts of very high temperature magma. Kilometre-scale buoyancy-driven convective stirring is, in general, unlikely to occur given current rheological models and heating rates. In addition, buoyancy-driven extraction of melt at low melt fraction appears to be a second-order process. Shear, extensional fracturing or some other mechanism appears to be required to achieve significant melt extraction.

6. Acknowledgements

We gratefully acknowledge Jim Quick, Alberto Patiño Douce, and Silvano Sinigoi for many fruitful discussions and assistance with the ongoing field studies. The editorial assistance of E-An Zen and comments from two reviewers is also gratefully acknowledged. Partial funding for this work was provided by NSF grant 9508291, a Royalty Research Fund grant from the University of Washington, and a AWU Faculty Fellowship to Battelle, Pacific Northwest Laboratory.

7. References

Agarwal, P. K. & O'Neill, B. K. 1988. Transport phenomena in multi-particle system—I. Pressure drop and friction factors: unifying the hydraulic-radius and submerged-object approaches. CHEM ENG SCI **43**, 2487–99.

Arzi, A. A. 1978. Critical phenomena in the rheology of partially melted rocks. TECTONOPHYSICS **44**, 173–84.

Barboza, S. A. 1995. *The dynamics of dehydration melting and implications for melt extraction in the lower crust following underplating: an example from the Ivrea-Verbano Zone, northern Italy*. M.S. Thesis, University of Washington.

Beard, J. S. & Lofgren, G. E. 1989. Effects of water on the composition of partial melts of greenstone and amphibolite. SCIENCE **244**, 195–7.

Beckermann, C. & Viskanta, R. 1988. Double-diffusive convection during dendritic solidification of a binary mixture. PHYSIOCHEM HYDRODYN **10**, 195–213.

Bennon, W. D. & Incropera, F. P. 1987. A continuum model for momentum, heat and species transport in binary solid–liquid phase change systems-I. Model formulation. INT J HEAT MASS TRANSFER **30**, 2161–70.

Bergantz, G. W. 1989. Underplating and partial melting: implications for melt generation and extraction. SCIENCE **245**, 1093–5.

Bergantz, G. W. 1995. Changing techniques and paradigms for the evaluation of magmatic processes. J GEOPHYS RES **100**, 17, 603–13.

Bergantz, G. W. & Dawes, R. 1994. Aspects of magma generation and ascent in continental lithosphere. *In* Ryan, M.P. (ed.) *Magmatic systems*, 291–317. San Diego: Academic Press.

Boriani, A., Bigioggero, B. & Origoni Giobbi, E. 1977. Metamorphism, tectonic evolution, and tentative stratigraphy of the 'Serie dei Laghi'—geological map of the Verbania Area (Northern Italy). MEM IST GEOL MINERAL UNIV PADOVA **32**, 1–25.

Boriani, A., Burlini, L., Caironi, V., Origoni, E. G., Sassi, A. & Sesana, E. 1988. Geological and petrological studies on the Hercynian plutonism of Serie dei Laghi—geological map of its occurrence between Valsesia and Lago Maggiore (N-Italy). REND SOC ITAL MINERAL PETROL **43–2**, 367–84.

Bowers, J. R., Kerrick, D. M. & Furlong, K. P. 1990. Conduction model for the thermal evolution of the Cupsuptic aureole, Maine. AM J SCI **290**, 644–65.

Brown, G. C. & Fyfe, W. S. 1970. The production of granitic melts during ultrametamorphism. CONTRIB MINERAL PETROL **28**, 310–8.

Brown, M. 1994. The generation, segregation, ascent and emplacement of granite magma: the migmatite-to-crustally-derived granite connection in thickened orogens. EARTH SCI REV **36**, 83–130.

Brown, M., Averkin, Y. A., McLellan, E. L. & Sawyer, E. W. 1995. Melt segregation in migmatites. J GEOPHY RES **100**, 15, 655–79.

Buntebarth, G. 1991. Thermal models of cooling. *In* Voll, G., Topel, J., Pattison, D.R.M. and Seifert, F. (eds.) *Equilibrium and kinetics in contact metmorphism: the Ballachulish Igneous Complex and its aureole*, 379–404, Heidelberg: Springer-Verlag.

Clemens, J. D. & Mawer, C. K. 1992. Granitic magma transport by fracture propagation. TECTONOPHYSICS **204**, 339–60.

Davison, I., McCarthy, M., Powell, D., Torres, H. H. F. & Santos, C. A. 1995. Laminar fow in shear zones: the Pernambuco Shear Zone, NE Brazil. J STRUCT GEOL **17**, 149–61.

Fountain, D. M. 1976. The Ivrea Verbano and Strona Ceneri zones, northern Italy, a cross-section of the continental crust: new evidence from seismic velocities of rock samples. TECTONOPHYSICS **33**, 145–65.

Fyfe, W. S. 1973. The granulite facies, partial melting and the Archean crust. PHIL TRANS R SOC LONDON SER A **273**, 457–61.

Giese, P. 1968. Die Struktur der Erdkruste im Bereich der Ivrea-Zone. Ein Vergleich verschiedener, seismischer Interpretationen und der Versuch einer petrographisch-geologischen Deutung. SCHWEIZ MINERAL PETROGR MITT **48**, 261–84.

Ghiorso, M. S. & Sack, R. O. 1995. Chemical mass transfer in magmatic processes IV. A revised and internally consistent thermodynamic model for the interpolation and extrapolation of liquid–solid equilibria in magmatic systems at elevated temperatures and pressures. CONTRIB MINERAL PETROL **119**, 197–212.

Grant, J. A. & Frost, B. R. 1990. Contact metamorphism and partial melting of pelitic rocks in the aureole of the Laramie anorthosite complex, Morton Pass, Wyoming. AM J SCI **290**, 425–72.

Harris, N., Ayres, M. & Massey, J. 1995. Geochemistry of granitic melts produced during the incongruent melting of muscovite: implications for the extraction of Himalayan leucogranite magmas. J GEOPHYS RES **100**, 15,767–77.

Huppert, H. E. & Sparks, R. S. J. 1988. The generation of granitic magmas by intrusion of basalt into continental crust. J PETROL **29**, 599–624.

Huppert, H. E. & Sparks, R. S. J. 1991. Comments on 'On convective style and vigor in sheetlike magma chambers' by Bruce D. Marsh. J PETROL **32**, 851–4.

Hyndman, D. W. 1981. Controls on source and depth of emplacement of granitic magma. GEOLOGY **9**, 244–9.

Irvine, T. N. 1970. Heat transfer during solidification of layered intrusions. I. Sheets and Sills. CAN J EARTH SCI **7**, 1031–61.

Jaupart, C. & Tait, S. 1995. Dynamics of differentiation in magma reservoirs. J GEOPHYS RES **100**, 17, 615–36.

Kay, R. W. & Kay, S. M. 1980. Chemistry of the lower crust: inferences from magmas and xenoliths. In National Research Council. Geophysics Study Committee (eds) *Continental Tectonics*, 139–50 Washington DC: National Academy of Sciences.

Kissling E. 1980. *Krustenaufbau und Isostasie in der Schweiz*. Ph.D. Thesis, ETH, Zurich.

Le Breton, N. & Thompson, A. B. 1988. Fluid-absent (dehydration) melting of biotite in metapelites in the early stages of anatexis. CONTRIB MINERAL PETROL **99**, 226–37.

Litvinovsky, B. A. & Podladchikov, Y. Y. 1993. Crustal anatexis during the influx of mantle volatiles. LITHOS **30**, 93–107.

Marsh, B. D. 1981. On the crystallininty, probability of occurrence and rheology of lava and magma. CONTRIB MINERAL PETROL **78**, 85–98.

Marsh, B. D. 1991. Reply to comments of Huppert and Sparks. J PETROL **32**, 855–60.

Mehnert, K. R. 1968. *Migmatites and the origin of granitic rocks*, 335–42. Amsterdam: Elsevier.

Mehnert, K. R. 1975. The Ivrea zone, a model of the deep crust. N JAHRB MINERAL ABH **125**, 156–99.

Miller, C. F., Watson, E. B. & Harrison, T. M. 1988. Perspectives on the source, segregation and transport of granitoid magmas. TRANS R SOC EDINBURGH: EARTH SCI **79**, 135–56.

Ni, J. & Beckermann, C. 1991. A volume-averaged two-phase model for transport phenomena during solidification. MET TRANS B **22**, 349–61.

Nicolas, A. 1989. *Structures of ophiolites and dynamics of ocean lithosphere*, 367. Dordrecht: Kluwer Academic.

Oldenburg, C. M. & Spera, F. J. 1991. Numerical modeling of solidification and convection in a viscous pure binary eutectic system. INT J HEAT MASS TRANSFER **34**, 2107–21.

Oldenburg, C. M. & Spera, F. J. 1992. Hybrid model for solidification and convection. NUMER HEAT TRANSFER B **21**, 217–29.

Patiño Douce, A. E. & Johnston, A. D. 1990. Phase equilibria and melt productivity in the pelitic system: implications for the origin of peraluminous granitoids and aluminous granulites. CONTRIB MINERAL PETROL **107**, 202–18.

Pitcher, W. S. 1993. The Origin of Granite, 321. Glasgow: Blackie Academic.

Prakash, C. & Voller, V. R. 1989. On the numerical solution of continuum mixture model equations describing binary solid-liquid phase change. NUMER HEAT TRANSFER B **15**, 171–89.

Quick, J. E., Sinigoi, S. & Mayer, A. 1994. Emplacement dynamics of a large mafic intrusion in the lower crust, Ivrea-Verbano Zone, northern Italy. J GEOPHYS RES **99**, 21,559–73.

Rivalenti, G., Garuti, G. & Rossi, A. 1975. The origin of the Ivrea-Verbano basic formation (Western Italian Alps)—whole rock geochemistry. BOLL SOC GEOL ITAL **94**, 1149–86.

Rivalenti, G., Garuti, G., Rossi, A., Siena, F. & Sinigoi, S. 1980. Existence of different peridotite types and of a layered igneous complex in the Ivrea-zone of the Western Alps. J PETROL **22**, 127–53.

Rushmer, T. 1991. Partial melting of two amphibolites: contrasting experimental results under fluid-absent conditions. CONTRIB MINERAL PETROL **107**, 41–59.

Rushmer, T. 1995. An experimental deformation study of partially molten amphibolite: application to low-melt fraction segregation. J GEOPHYS RES **100**, 15,681–95.

Rutter, E. H. & Neumann, D. H. K. 1995. Experimental deformation of parially moten Westerly granite under fluid-absent conditions, with implications for the extraction of granitic magmas. J GEOPHYS RES **100**, 15,697–715.

Sawyer, E. W. 1991. Disequilibrium melting and the rate of melt-residuum separation during migmatization of mafic rocks from the Grenville Front, Quebec. J PETROL **32**, 701–38.

Sawyer, E. W. 1994. Melt segregation in the continental crust. GEOLOGY **22**, 1019–22.

Schnetger, B. 1994. Partial melting during the evolution of the amphibolite-to granulite-facies gneisses of the Ivrea Zone, northern Italy. CHEM GEOL **113**, 71–101.

Schmid, R. 1978/79. Are the metapelites of the Ivrea-Verbano Zone restites? MEM IST GEOL MINERAL UNIV PADOVA **33**, 67–9.

Schmid, S. M. & Wood, B. J. 1976. Phase relationships in granulitic metapelites from the Ivrea–Verbano zone. CONTRIB MINERAL PETROL **54**, 255–79.

Schmid, S. M., Zingg, A. & Handy, M. 1987. The kinematics of movements along the Insubric Line and the emplacement of the Ivrea Zone. TECTONOPHYSICS **135**, 47–66.

Schulze, F., Behrens, H. & Holtz, F. 1994. Effect of water on the viscosity of haplogranitic melts. Experimental investigation using the falling sphere method. EOS, TRANS AM GEOPHYS UNION **75** (44), 724.

Shaw, H. R. 1972. Viscosities of magmatic liquids: an empirical method of prediction. AM J SCI **272**, 870–93.

Sills, J. D. & Tarney, J. 1984. Petrogenesis and tectonic significance of amphibolites interlayered with meta-sedimentary gneisses in the Ivrea Zone, Southern Alps, NW Italy. TECTONOPHYSICS **107**, 187–206.

Sinigoi, S., Quick, J. E., Clemens-Knott, D., Mayer, A., Dimarchi, G., Mazzucchelli, M., Negrini, L. & Rivalenti, G. 1994. Chemical evolution of a large mafic intrusion in the lower crust, Ivrea-Verbano Zone, northern Italy. J GEOPHYS RES, **99**, 21,575–90.

Sinton, J. M. & Detrick, R. S. 1992. Mid-ocean ridge magma chambers. J GEOPHYS RES **97**, 197–216.

Swanson, D. A., Cameron, K. A., Evarts, R. C., Pringle, P. T. & Vance, J. A. 1989. Cenozoic volcanism in the Cascade Range and Columbia Plateau, southern Washington and northermost Oregon. NEW MEXICO BUR MINES MINERAL RES MEM **47**, 1–50.

Symmes, G. H. & Ferry, J. M. 1995. Metamorphism, fluid flow and partial melting in pelitic rocks from the Onawa contact aureole, central Maine, USA. J PETROL **36**, 587–612.

Thompson, A. B. 1982. Dehydration melting of pelitic rocks and the generation of H_2O–undersaturated granitic liquids. AM J SCI **282**, 1567–95.

van der Molen, I. & Paterson, M. S. 1979. Experimental deformation of partially-melted granite. CONTRIB MINERAL PETROL **70**, 299–318.

Vielzeuf, D. & Holloway, J. R. 1988. Experimental determination of the fluid-absent melting relations in the pelitic system. CONTRIB MINERAL PETROL **98**, 257–76.

Whitney, J. A. 1988. The origin of granite: the role and source of water in the evolution of granitic magmas. GEOL SOC AM BULL **100**, 1886–97.

Wickham, S. M. 1987. The segregation and emplacement of granitic magmas. J GEOL SOC LONDON **144**, 281–97.

Wildemuth, C. R. & Williams, M. C. 1984. Viscosity of suspensions modeled with a shear dependent maximum packing fraction. RHEOL ACTA **23**, 627–35.

Wyllie, P. J. 1977. Crustal anatexis: an experimental review. TECTONOPHYSICS **43**, 41–71.

Yardley, B. W. D. 1986. Is there water in the deep continental crust? NATURE **323**, 111.

Zingg, A. 1980. Regional metamorphism in the Ivrea Zone (Southern Alps, N-Italy): field and microscopic investigations. SCHWEIZ MINERAL PETROGR MITT **60**, 153–79.

Zingg, A. 1983. The Ivrea and Strona-Ceneri Zones (Southern Alps, Ticino and North Italy): a review. SCHWEIZ MINERAL PETROGR MITT **63**, 361–92.

SCOTT A. BARBOZA and GEORGE W. BERGANTZ, Department of Geological Sciences and Volcano Systems Center, Box 351310, University of Washington, Seattle, WA 98195, U.S.A.
E-mail: barboza@u.washington.edu